Drop of Thermal Contacts Resistance between Multi-Layer Graphene and Metals caused by Laser

Victor A. Ermakov[1], Alfredo R. Vaz[1], Andrei V. Alaferdov[1] and Stanislav A. Moshkalev[1]

[1] Center for Semiconductor Components, State University of Campinas, CP 6101,
Campinas, SP, 13083-870, Brazil
e-mail: victor.ermakov@ccs.unicamp.br

ABSTRACT

Significant drop of thermal contact resistance between a graphene flake and metal electrodes was shown as a result of laser annealing. The improvement of thermal contacts of initially rough metal electrodes is attributed to local melting of the metal surface caused by laser heating followed by increasing of real metal-graphene contact area.

Index Terms: graphene; thermal contact; laser annealing

I. INTRODUCTION

Potential applications of graphene for thermal management in electronic devices are very promising as in-plane thermal conductivity of single layer graphene is extremely high, up to $5x10^3$ $Wm^{-1}K^{-1}$ [1]. A number of techniques was used to measure thermal conductivity K of a single layer, a few-layer, multi-layer graphene (SLG, FLG and MLG, respectively) [2-8]. However, the precision of K measurements can be affected by poor thermal contacts between graphene and metal electrodes. Heat transfer through contacts and interfaces between nanostructured materials is an important issue in nanoelectronics, in studies of nanocomposites and thermal interface materials, but it is still poorly understood and the existing models of electrical and thermal contacts are often inapplicable at the nanoscale.

In conventional electronic devices, interfaces between two thermally dissimilar materials like metals and semiconductors are assumed to be planar and perfectly matched. In reality, the contact thermal resistance between nanostructured materials is determined by two factors: the overlap of phonon states for two solids and the properties of the interface itself (roughness, adhesion between materials). The heat transfer between two solids in a perfect contact (strong bond) can be calculated using diffusive mismatch model or acoustic mismatch model (DMM or AMM, respectively) [9,10]. The efforts to improve the thermal interface models continue [11-13], however, the existing models are based on various simplifying assumptions and often fail to describe real nanoscale systems composed by materials with large differences in mechanical and thermal properties. In particular, graphene materials are characterized by extremely high anisotropy (in-plane / cross-plane) and large vibrational mismatch with most solid materials used in nanoelectronics (metals, oxides), so theoretical predictions of thermal transport between these materials are difficult.

High-quality thermal contacts between graphene and metals usually are obtained using conventional high-temperature annealing in vacuum. However, as shown in our previous study [14], this can induce strain in multi-layer graphene due to formation of tight mechanical contacts between graphene and metal electrodes followed by the electrodes shrinkage, and thus stretching the graphene flake. Therefore, it is desirable to perform annealing by heating locally the graphene flake and the area of contacts, without substantial heating of the electrode bodies. In this paper we continue our study of improving thermal contact resistance between graphene and metal contacts and focus on results of local contact annealing that was achieved by using laser. The dramatic effect of localized laser thermal annealing for improving of thermal contacts between graphene and metals or silicon oxide was shown. Heating caused by the laser leads to, eventually, mild "welding" of the graphene to the initially rough metal surface. In the present work we showed also that conventional micro-Raman technique can be applied for determination of temperature at which the electrode local melting occures. Also we calculated thermal conductivity in direction along suspended multi-layer graphene flakes using Raman measurement results as proposed previously in [1].

II. EXPERIMENTAL

Multi-layer graphene flakes were prepared by mild ultrasound processing (sonication) of natural graphene flakes (Nacional de Grafite Ltda, Brazil) in N,N-dimethylformamide (DMF) solutions. Most of graphene flakes had lateral dimensions in the range from 1 to 10 μm, and the thickness from 10 to 100 nm, as revealed by SEM (scanning electron microscope) observations. Further, the MLG flakes were deposited over metal (Au, Ti or W) electrodes with 1 μm separation using ac di-electrophoresis [14]. Electrodes with thickness of 100 nm and surface roughness of 1-2 nm were deposited over thermally oxidized Si (oxide thickness of about 300 nm) by plasma sputtering using conventional photolithography and lift-off processes. The micron size trenches (1 μm wide and 5 μm deep) between electrodes were previously cut by focused ion beam (Nova 200 Nanolab, FEI Co). A 473 nm laser focused on the sample with 100x objective (~400 nm diameter laser spot, max laser power at the sample of 10 mW) was used for confocal Raman spectroscopy (Ntegra Spectra, NT MDT). In Raman spectra, narrow graphene G-lines (peak near 1580 cm^{-1} and FWHM ~15 cm^{-1}) and low-intensity D-lines (peak near 1360 cm^{-1}) were detected, indicating high quality of MLG flakes obtained by liquid phase exfoliation from natural graphite.The optothermal micro-Raman method [1] is based on measurements of the frequency downshift ΔG of a graphene G-line with increasing temperature (in some cases, 2D line is used). Note that the same laser was used for local heating of suspended graphene samples (duration of annealing varied between 1 and 10 sec in different experiments) and, simultaneously, for local graphene temperature measurements in situ (). From the measured ΔG value, the local graphene temperature rise ΔT above room temperature can be estimated, using the conversion coefficient that was measured to be -0.011 $cm^{-1}K^{-1}$ for multi-layer graphene [15].

III. RESULTS AND DISCUSSION

Examples of MLG deposited over various metal (W, Ti, Au) electrodes forming side contacts with the metal are shown in Fig. **1**.

The G-line position was found first to shift linearly with laser power (see Fig. **2**) indicating gradual heating of the sample proportional to the absorbed power, as expected. However, with increasing power the shift was found to saturate or even reduce.

We recalculated G-line shift into the temperature using procedure described in [1] for flakes deposited over Au and W electrodes (see Fig. **3**):

$$\Delta T\ (K) = \Delta\omega\ (cm^{-1})\ /\ g\ (cm^{-1}K^{-1})$$

Using conversion coefficient g = -0.011 $cm^{-1}K^{-1}$, very high local graphene temperatures (from 900K) can be estimated from the maximum G-line

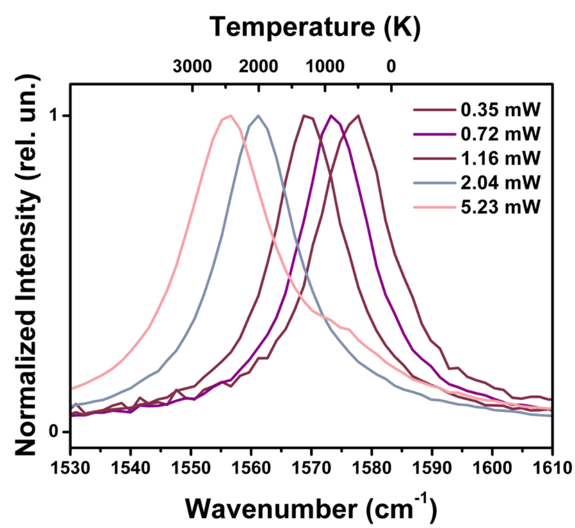

Figure 2. Shift of G-peak position caused by laser heating with different laser power for graphene flake deposited over W electrodes. Position of a maximum of G-peak corresponds to a temperature of the flake (shown on the top axis).

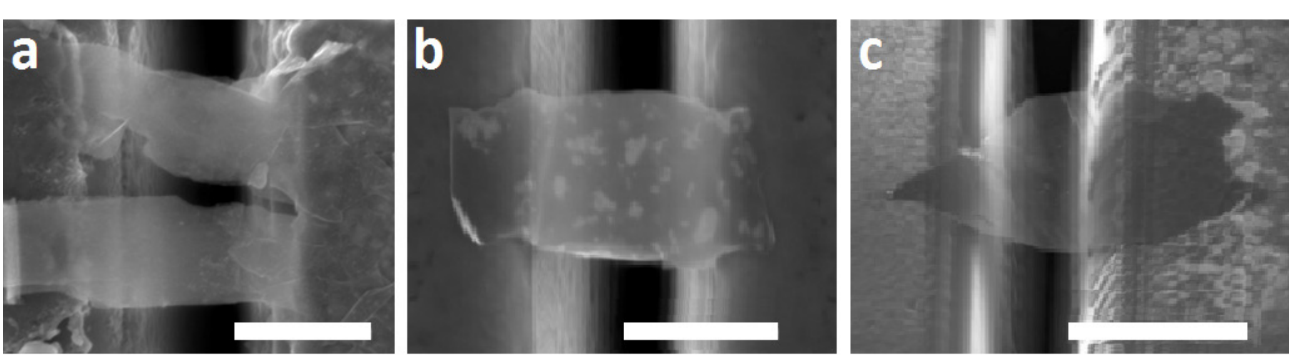

Figure 1. SEM images of multi-layer graphene flakes deposited over a) - W, b) - Ti and c) - Au electrodes. White bars correspond to 5 μm.

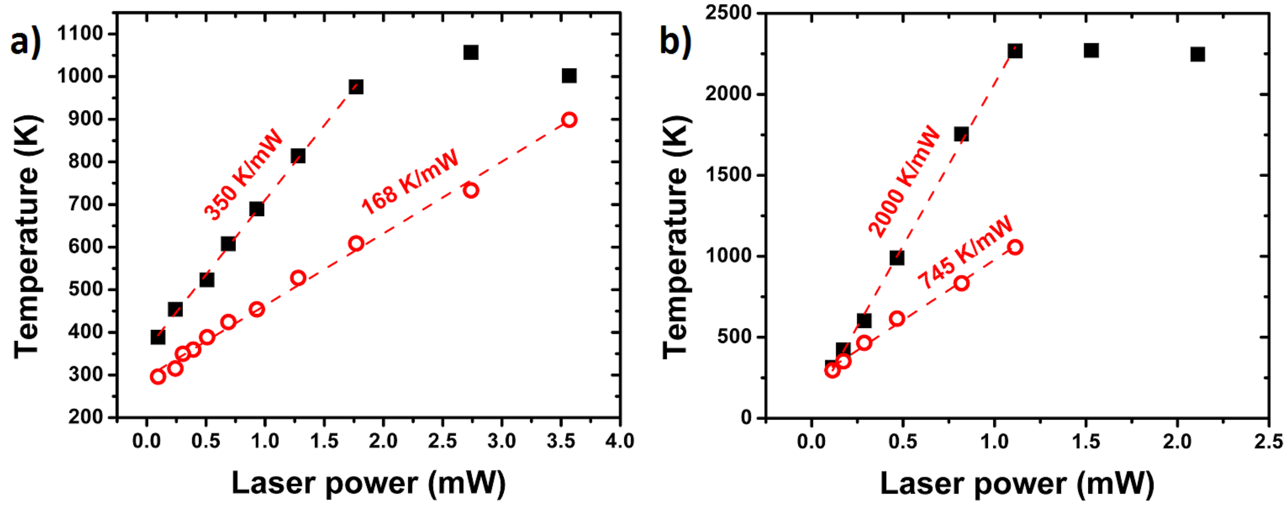

Figure 3. Laser heating of graphene on Au (a) and W (b) contacts. Dashed line (average slope) shows thermal resistance between contact surfaces.

downshifts. For different cases the maximum temperature was found to vary between 930K and 2300K for laser power up to 10 mW, depending on the flake dimensions and quality of contact with electrodes. The smallest downshifts were obtained for Au electrodes with the largest contact area. In the case shown in Fig. **3**.a (on Au electrodes), the saturation occurs at approximately 1000K. The effect of saturation can be attributed to improvement of the thermal contact between the MLG and metal electrode that can occur during sample heating, resulting in increased heat losses to the electrodes and, finally, in the reduced sample temperature. This is confirmed by results obtained in the second run performed immediately after the first one (Fig. **3**, red circles), when much lower graphene temperatures (G-line downshifts) are detected for the same laser powers, with the curve slope of 168 K/mW, as compared with 350 K/mW for the first run, in the case of Au electrode (Fig. **3**,a).

Heat losses from the graphene surface due to thermal contact with air (~10^5 $Wm^{-2}K^{-1}$) [16] and by radiation are estimated to be much smaller than the absorbed laser power (~0.1 mW and 10^{-8} mW, respectively). Thus under the present conditions the main mechanism of heat losses is due to heat transfer through the graphene-metal contacts, and the reduced sample heating during the second run clearly indicates the improved thermal conductivity of the graphene-metal contact (thermal boundary conductance) after annealing occurred during the first run. The thermal contact improvement is likely due to partial melting of the metal surface in contact with graphene, reducing of the initially high metal surface roughness under the graphene and corresponding increase of the contact area and adhesion between surfaces (). This is possible because of distinctly different mechanical properties of two contacting materials: (i) multi-layer graphene with a perfectly flat surface, characterized by high in-plane elastic stiffness and high cross-plane hardness, and (ii) rough metal surface that is subject to plastic deformation at nanoscale length under pressure (due to adhesion) and heat flow. Note that lower temperatures obtained for Au electrodes () can be due to higher self-diffusion of this metal under heating, compared with other metals tested here (W,Ti).

The thermal boundary conductance (TBC) of the interface between different metals was estimated from the experimental data obtained with local laser heating of MLG to be ~30-50 $MWm^{-2}K^{-1}$ for metals like Au, Ti and W. The maximum TBC values were found after laser annealing at elevated laser power.

The maximum values of thermal conductivity obtained for narrow multi-layer graphene samples after annealing were found to be close to 600 $Wm^{-1}K^{-1}$ (consistent with data in literature for flakes with re-

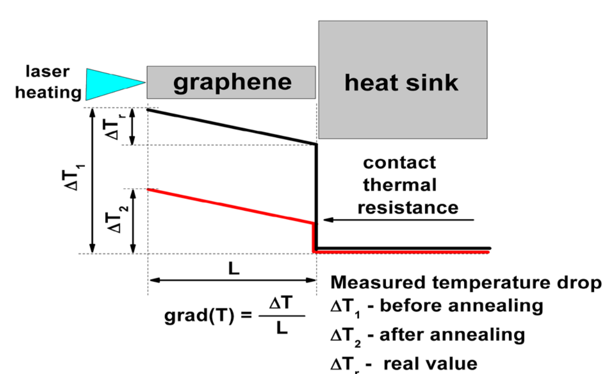

Figure 4. Schematics of the temperature distribution along the graphene before (black) and after the laser annealing of contacts with electrode.

duced lateral dimensions) compared with much lower values <150 $Wm^{-1}K^{-1}$ obtained without annealing [17]. This finding shows the importance of establishing good thermal contacts between graphene and metals for thermal characterization of carbon nanostructured materials such as graphene and nanotubes.

IV. CONCLUSIONS

We registered a more than-two-times drop of thermal contacts resistance between multi-layer graphene and metal contacts caused by laser annealing. Based on the presented above experimental results, the following conclusions can be made: high-temperature (T ~ 1000 °C) local annealing is necessary to achieve reasonable quality of contacts with metal surfaces that are usually relatively rough (although the degree of roughness may depend on the metal deposition method). Significant improvement of contacts between multi-layer graphene and various metal electrodes by local laser annealing has been successfully demonstrated in the present work. In contrast to a conventional thermal annealing, the great advantage of the local laser annealing is that substrate heating in the case is not necessary. The improvement of contacts can be also attributed to removal of air pockets, solvent traces and other possible impurities. Experiments are currently in progress to perform laser annealing under vacuum conditions, where considerably higher local temperatures and better contacts could be achieved without any possible damaging of the graphene.

ACKNOWLEDGEMENTS

The authors would like to acknowledge CNPq, FAPESP, INCT NAMITEC for financial support, CCS-UNICAMP staff for technical assistance, Dr. Raluca Savu and Angelo Gobbi (LNLS, Campinas) for help in preparation of samples.

REFERENCES

[1] A.A. Balandin, S. Ghosh, W. Bao, I. Calizo, D. Teweldebrhan, F. Miao and C.N. Lau "Superior Thermal Conductivity of Single-Layer Graphene," Nano Lett. vol. 8, pp. 902-907, 2008.

[2] W. Cai, A.L. Moore, Y. Zhu, X. Li, S. Chen, L. Shi and R.S. Ruoff 2010 Thermal Transport in Suspended and Supported Monolayer Graphene Grown by Chemical Vapor Deposition Nano Lett. 10 1645-51.

[3] C. Faugeras, B. Faugeras, M. Orlita, M. Potemski, R.R. Nair and A.K. Geim, "Thermal Conductivity of Graphene in Corbino Membrane Geometry," ACS Nano, vol. 4, pp. 1889-92, 2010.

[4] S. Ghosh, W. Bao, D.L. Nika, S. Subrina, E.P. Pokatilov, C.N. Lau and A.A. Balandin, "Dimensional crossover of thermal transport in few-layer graphene," Nat. Mater., vol. 9, pp. 555-8. 2010

[5] V. Vlassiouk, S. Smirnov, I. Ivanov, P.F. Fulvio, S. Dai, H. Meyer, M. Chi, D. Hensley, P. Datskos and N.V. Lavrik, "Electrical and thermal conductivity of low temperature CVD graphene: the effect of disorder," Nanotechnology, vol. 22, pp. 275716-9, 2011.

[6] J.-U. Lee, D. Yoon, H. Kim, S.W. Lee and H. Cheong, "Thermal conductivity of suspended pristine graphene measured by Raman spectroscopy," Phys. Rev. B, vol. 83, pp. 081419-4, 2011

[7] M.T. Pettes, I. Jo, Z. Yao and L. Shi, "Influence of Polymeric Residue on the Thermal Conductivity of Suspended Bilayer Graphene," Nano Lett., vol. 11, pp. 1195-200, 2011.

[8] T. Schwamb, B.R. Burg, N.C. Schirmer and D. Poulikakos, "An electrical method for the measurement of the thermal and electrical conductivity of reduced graphene oxide nanostructures," Nanotechnology, vol. 20, pp. 405704-4, 2009.

[9] G. Chen, Nanoscale Energy Transport and Conversion, NY: Oxford University Press, 2005.

[10] E.T. Swartz, R.O. Pohl, "Thermal boundary resistance," Rev. Mod. Phys., vol. 61, pp. 605-68, 1969.

[11] P.M. Norris, J.L. Smoyer, J.C. Duda and P.E. Hopkins, "Prediction and measurement of thermal transport across interfaces between isotropic solids and graphitic materials," J. Heat Transfer, vol. 134, pp. 020910-7, 2012.

[12] R. Prasher, "Acoustic mismatch model for thermal contact resistance of van der Waals contacts," Appl. Phys. Lett., vol. 94, pp. 041905-3, 2009.

[13] T. Beechem, J.C. Duda, P.E. Hopkins and P.M. Norris, "Contribution of optical phonons to thermal boundary conductance," Appl. Phys. Lett., vol. 97, pp. 061907-3, 2010.

[14] F.P. Rouxinol, R.V. Gelamo, R.G. Amici, A.R. Vaz and S.A. Moshkalev, "Low contact resistivity and strain in suspended multilayer graphene," Appl. Phys. Lett., vol. 97, pp. 253104-3, 2010.

[15] I. Calizo, F. Miao, W. Bao, C.N. Lau and A.A. Balandin, "Variable temperature Raman microscopy as a nanometrology tool for graphene layers and graphene-based devices," Appl. Phys. Lett., vol. 91, pp. 071913-3, 2007.

[16] I.-K. Hsu, M.T. Pettes, M. Aykol, L. Shi and S.B. Cronin, "The effect of gas environment on electrical heating in suspended carbon nanotubes," J. Appl. Phys., vol. 108, pp. 084307-5, 2010.

[17] V.A. Ermakov, A.V. Alaferdov, A.R. Vaz, A.V. Baranov and S.A. Moshkalev, "Nonlocal laser annealing to improve thermal contacts between multi-layer graphene and metals," Nanotechnology, vol. 24, pp. 155301-10.

[18] A.V. Alaferdov, R. Savu, M.A. Canesqui, A.R. Vaz, V.A. Ermakov, S.A. Moshkalev, "Study of the thermal contact between carbon nanotubes and a metal electrode", Journal of Surface Investigation: X-Ray, Synchrotron, and Neutron Techniques, vol.7, pp.607 - 611, 2013